

Supporting Information

for "Size-Controlled Pd Nanoparticle Catalysts Prepared by Galvanic Displacement into a Porous Si-Iron Oxide Nanoparticle Host."

Taeho Kim,^a Xin Fu,^b David Warther,^a and Michael J. Sailor^{*,a}

^a*Department of Chemistry and Biochemistry, University of California, San Diego, San Diego, USA*

^b*Department of Nanoengineering, University of California, San Diego, San Diego, USA*

*Corresponding author. E-mail: msailor@ucsd.edu

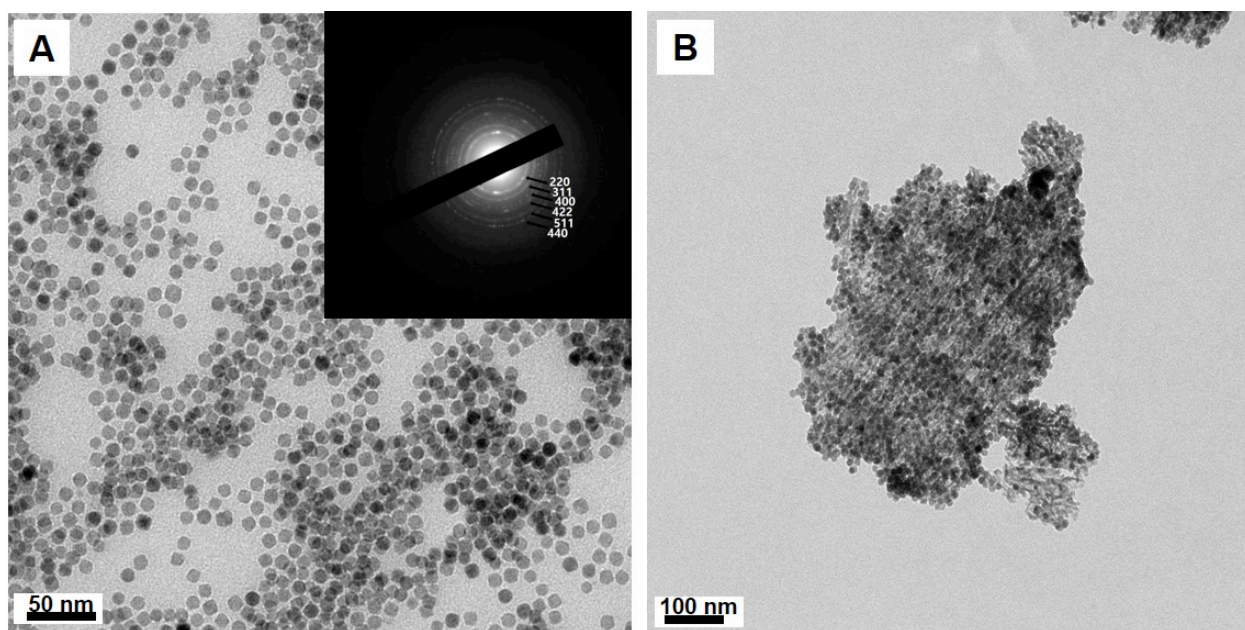


Figure S1. Transmission electron microscope (TEM) images of isolated γ -Fe₂O₃ nanoparticles (A) and composite nanoparticles consisting of γ -Fe₂O₃ nanoparticles trapped within a porous Si nanoparticle matrix (B). The γ -Fe₂O₃ nanoparticles in (A) show an average particle size (by DLS) of 7 nm. Inset of this (A) shows the selected area electron diffraction (SAED) pattern indexed with the cubic structure of the maghemite phase (JCPDS No. 39-1346) of iron oxide nanoparticles. The result of infiltration of γ -Fe₂O₃ nanoparticles into porous Si nanoparticles is referred to in this work as magnetic porous Si nanoparticles (MpSiNPs).

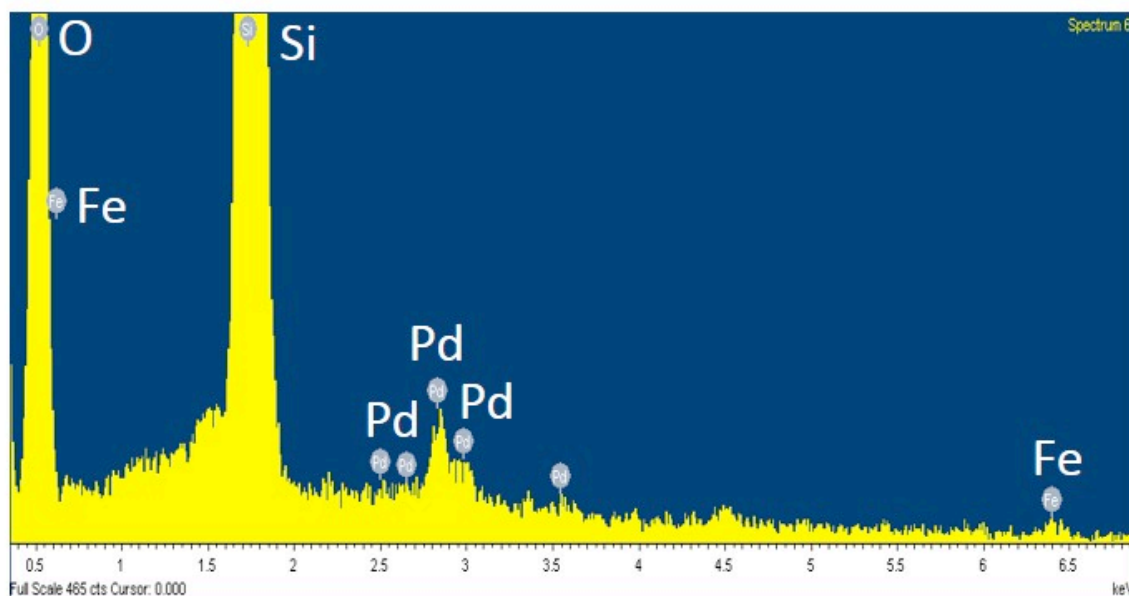


Figure S2. Energy-dispersed X-ray spectrum (EDS) of magnetic Pd-loaded porous Si nanoparticles (MpSi-PdNPs) prepared by sequential infiltration of γ -Fe₂O₃ nanoparticles and electroless deposition of Pd within a porous Si nanoparticle host. The coordination complex [Pd(NH₃)₄]²⁺ was used as the palladium source.

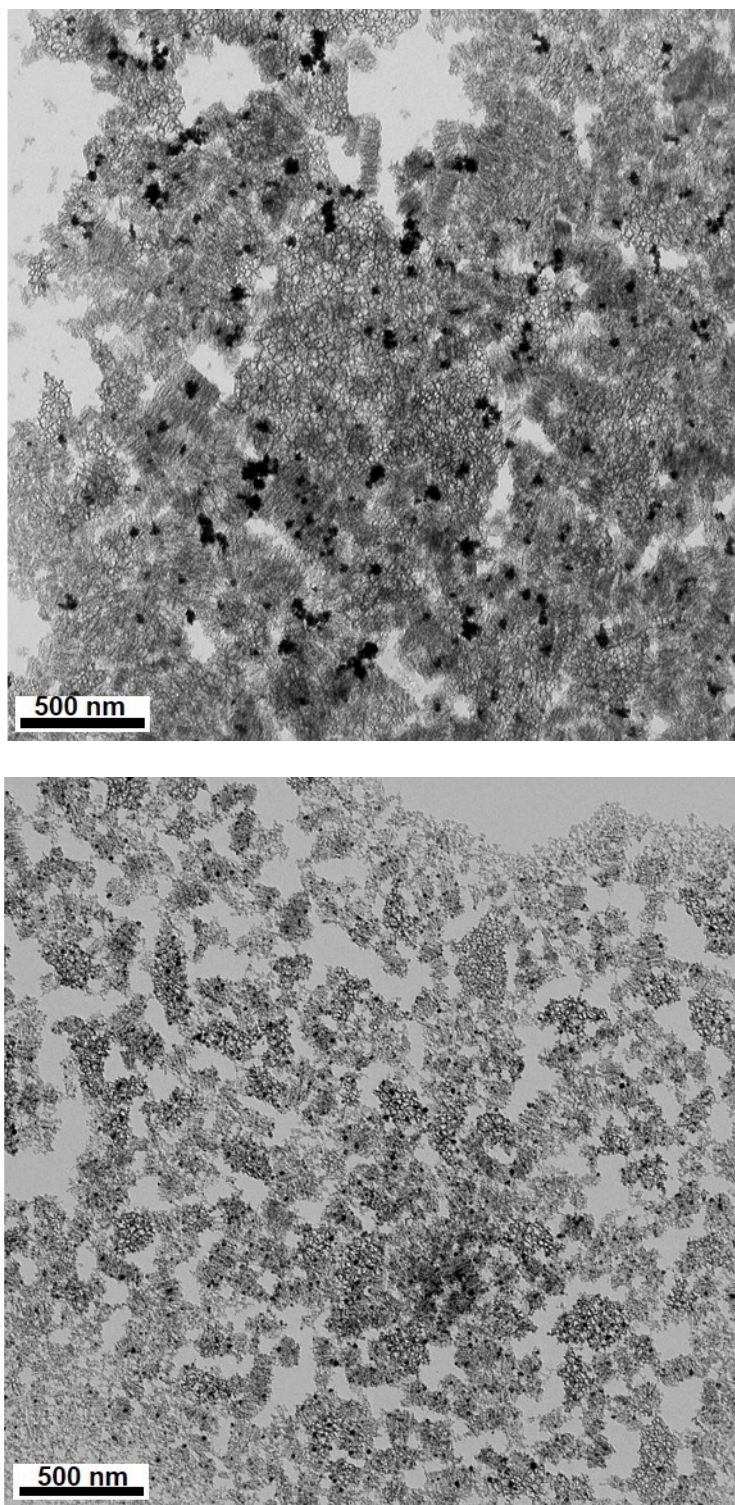


Figure S3. Low magnification TEM images of the result of Pd deposition within porous Si nanoparticles using aqueous PdCl₂ (top image) or [Pd(NH₃)₄]²⁺ (bottom image) as the palladium source.

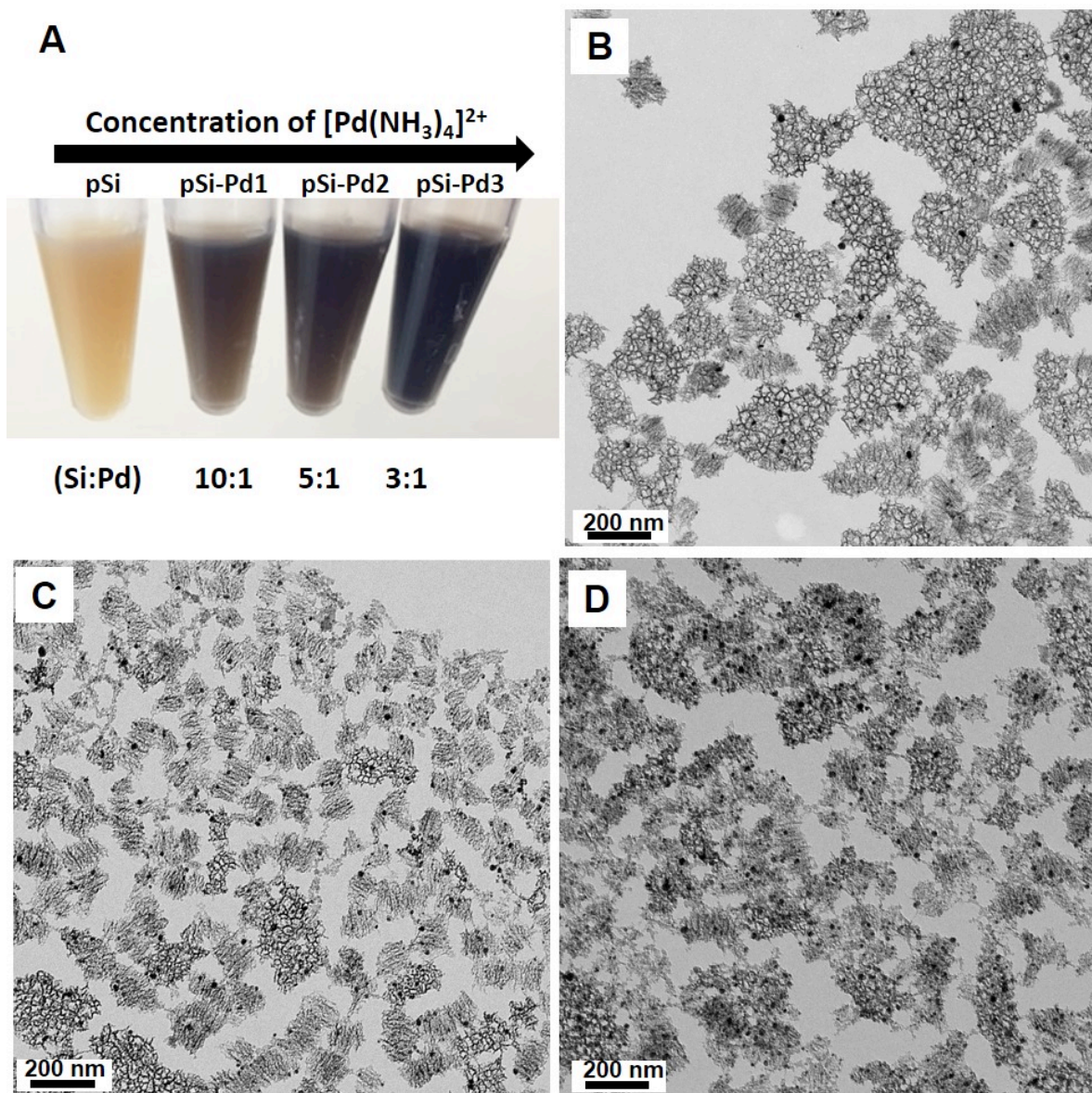


Figure S4. Photograph and TEM images of porous Si-Pd nanoparticles (pSi-PdNPs) prepared by introducing a given concentration of $[\text{Pd}(\text{NH}_3)_4]^{2+}$ solution to a set concentration of empty porous Si nanoparticles. (A) Photograph of pSi-PdNP suspensions prepared with increasing concentration of $[\text{Pd}(\text{NH}_3)_4]^{2+}$: 0, 1, 2, 4 μL of 0.1 M $[\text{Pd}(\text{NH}_3)_4]^{2+}$ solution, added to 0.2 mL of pSiNP (1 mg/mL) in deionized water. The Si to Pd mass ratio of the starting materials for the reaction is given below each vial. The vial on the far left is a control containing no Pd. The color of the nanoparticle solutions changes from yellow to dark brown to black with increasing Pd content. (B) TEM image of pSi-PdNPs with Si:Pd mass ratio of 10:1 (pSi-Pd1). (C) TEM image of pSi-PdNPs with Si:Pd mass ratio of 5:1 (pSi-Pd2). (D) TEM image of pSi-PdNPs with Si:Pd mass ratio of 3:1 (pSi-Pd3). Increasing the concentration of $[\text{Pd}(\text{NH}_3)_4]^{2+}$ solution increases the number density of Pd nanoparticles in the pSi matrix without substantially changing Pd nanoparticle size.

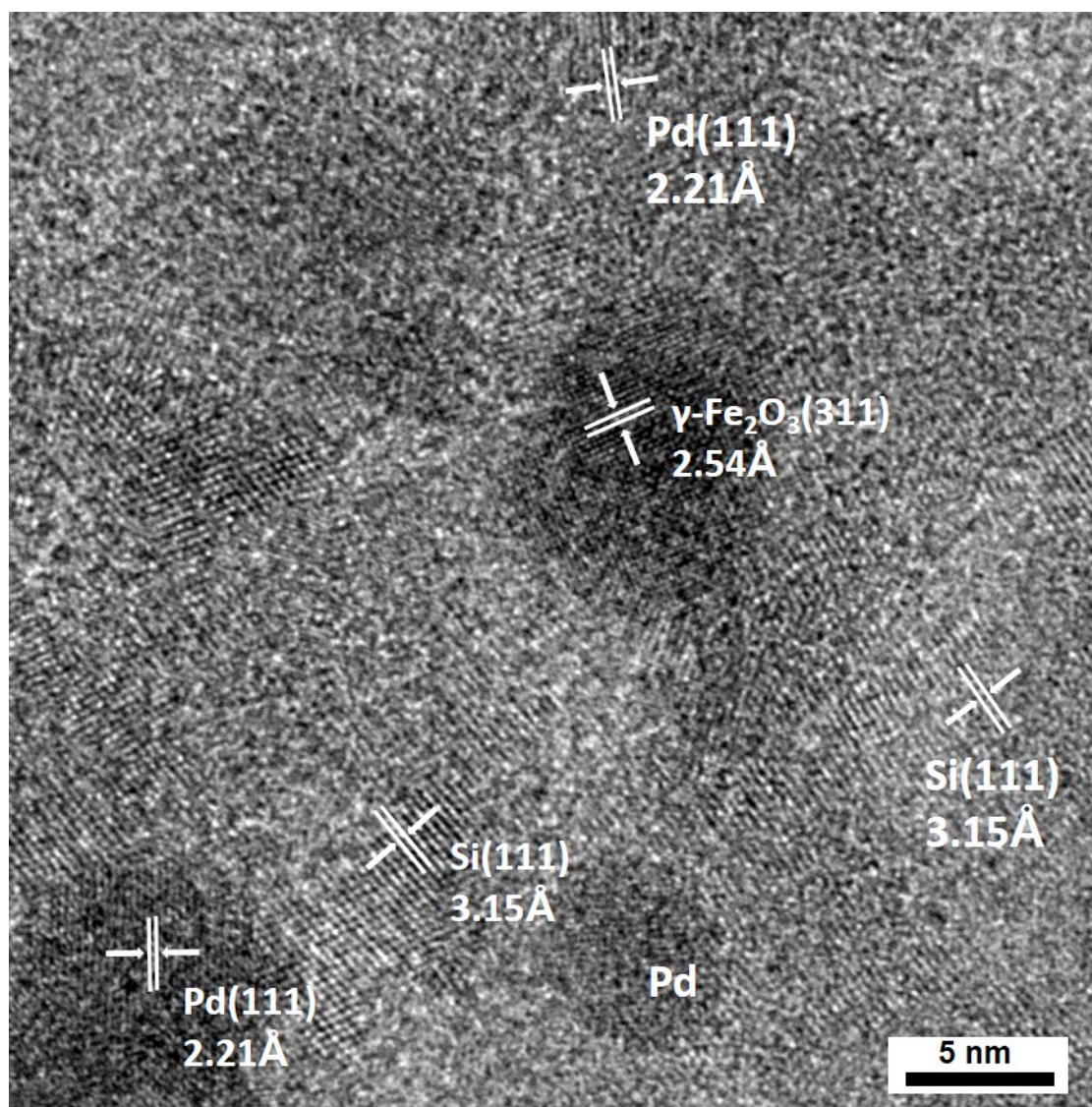


Figure S5. High-resolution TEM images of a single MpSi-Pd composite nanoparticle. All three nanoparticles are distinguishable, and the measured lattice spacings are: 3.15 Å, assigned to the (111) plane of Si; 2.54 Å, assigned to the (311) plane of $\gamma\text{-Fe}_2\text{O}_3$; and 2.21 Å, assigned to the (111) plane of Pd.

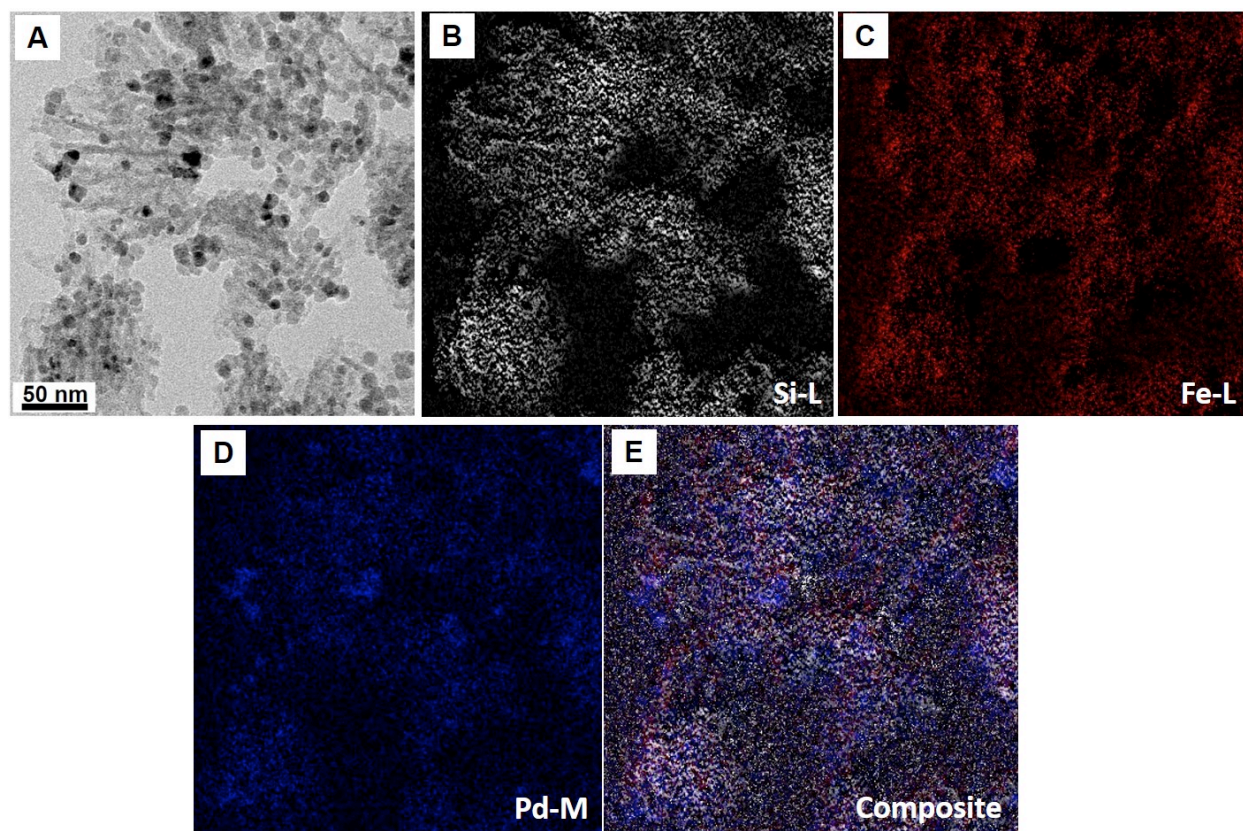


Figure S6. (A) TEM image of MpSi-Pd composite nanoparticles. (B)-(D) corresponding elemental maps of Si, Fe, and Pd derived from 2-dimensional energy-dispersive X-ray spectroscopy (EDS) maps. (E) overlay of images (B), (C), and (D).

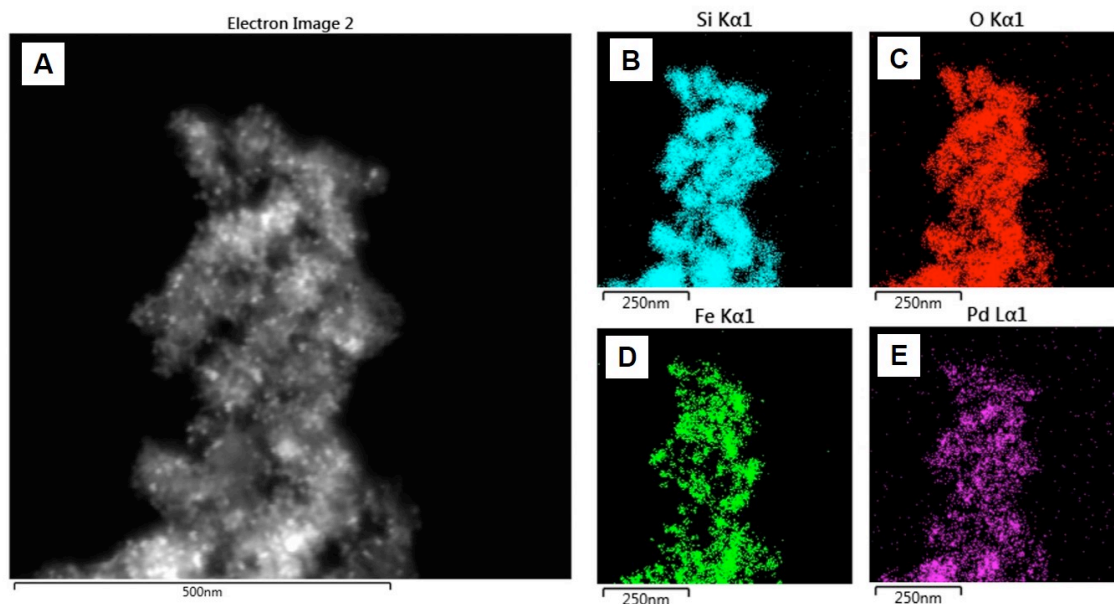


Figure S7. (A) High-angle annular dark-field (HAADF) STEM image of MpSi-Pd nanoparticles. (B)-(E) EDS elemental maps of the Si, O, Fe, and Pd signals as indicated.

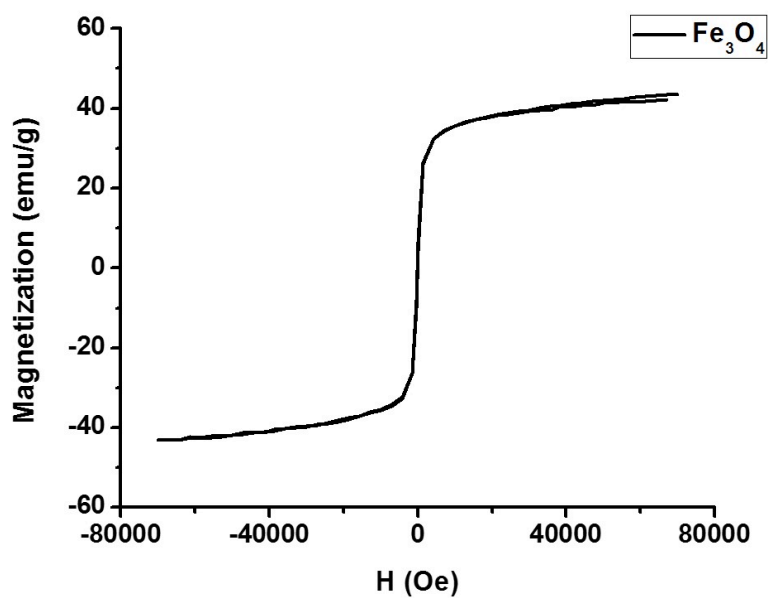


Figure S8. Magnetization curve (298 K) of $\gamma\text{-Fe}_2\text{O}_3$ nanoparticles used in this study. Saturation magnetization is 48 emu/g.

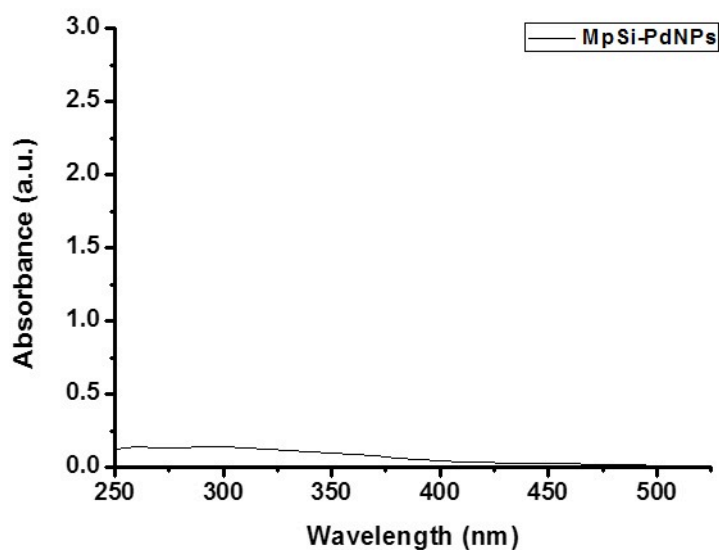


Figure S9. UV-Vis absorbance spectrum of the magnetic Pd-loaded porous Si nanoparticles (MpSi-PdNPs) used in this work, dispersed in deionized water. Nanoparticle concentration is comparable to that used in the catalytic reactions (see Figure 4 in the main text). The data show that at the concentrations used in the catalysis study, there is little spectral interference from nanoparticle absorbance.

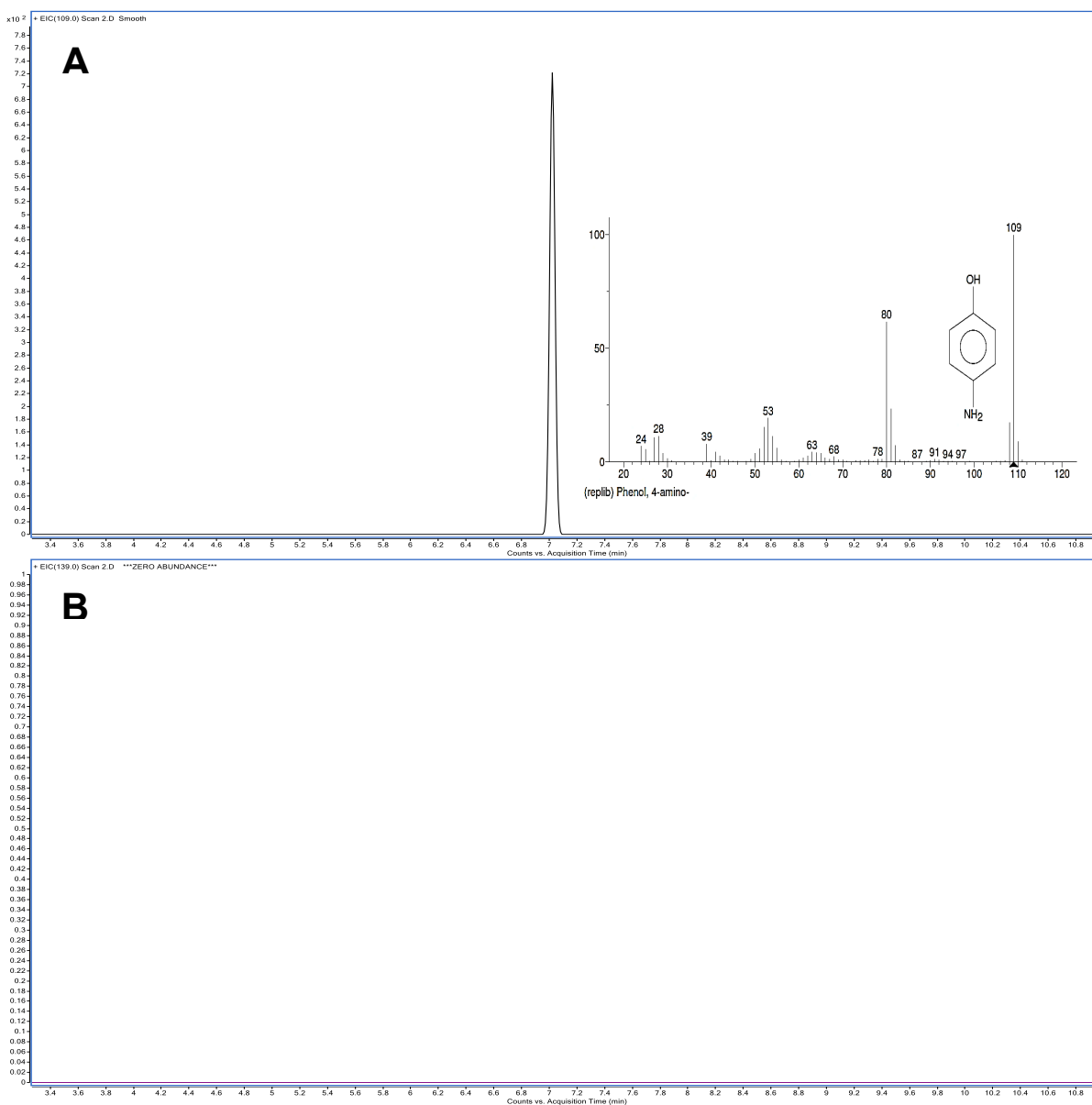


Figure S10. GC-MS analysis of catalytic reaction products. (A) The extracted ion chromatogram at $m/z = 109$. The M^+ peak is assigned to 4AP (C_6H_7NO). (B) The extracted ion chromatogram at $m/z = 139$. The M^+ peak is assigned to 4NP ($C_6H_5NO_3$). Inset of (A) shows the mass spectrum of the product.

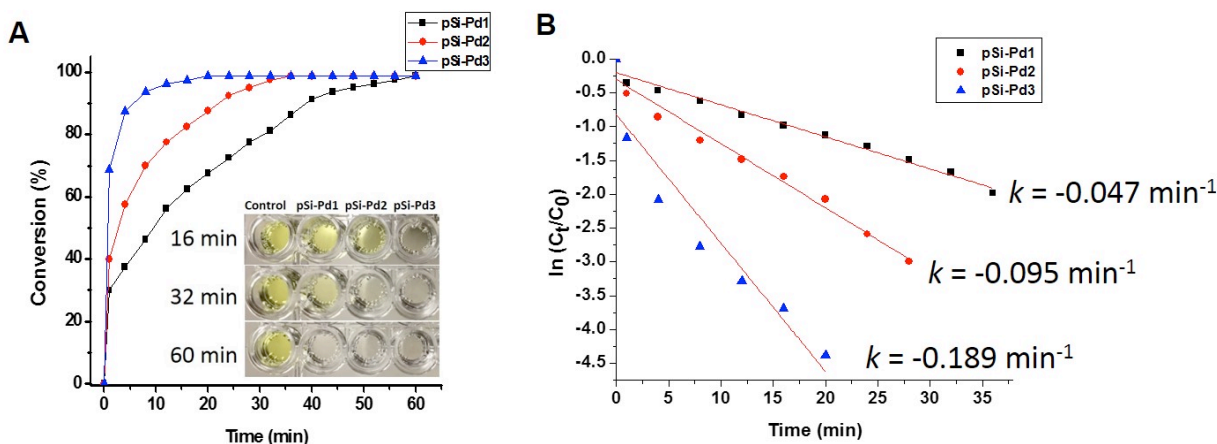


Figure S11. Effect of mass loading of Pd on the catalytic activity of Pd-loaded porous Si nanoparticles. The particles in this experiment were not loaded with $\gamma\text{-Fe}_2\text{O}_3$ nanoparticles and $[\text{Pd}(\text{NH}_3)_4]^{2+}$ was used as the Pd source. (A) Conversion of 4-nitrophenol (4NP) to 4-aminophenol (4AP) using the indicated Pd nanocomposite catalysts as a function of time: ■ pSi-Pd1 corresponds to Si:Pd mass ratio of 10:1; ● pSi-Pd2 corresponds to Si:Pd mass ratio of 5:1; ▲ pSi-Pd3 corresponds to Si:Pd mass ratio of 3:1. The inset shows photographs of the reaction at the indicated times after initiation. Control is empty porous Si nanoparticles (not loaded with Pd). (B) Plot of $\ln(C_t/C_0)$ versus time for the reduction of 4NP in the presence of the indicated Pd nanoparticle catalysts. The rate constant k is determined from the slope of the least-squares fit line. All experiments contained the same total mass of composite nanoparticle.

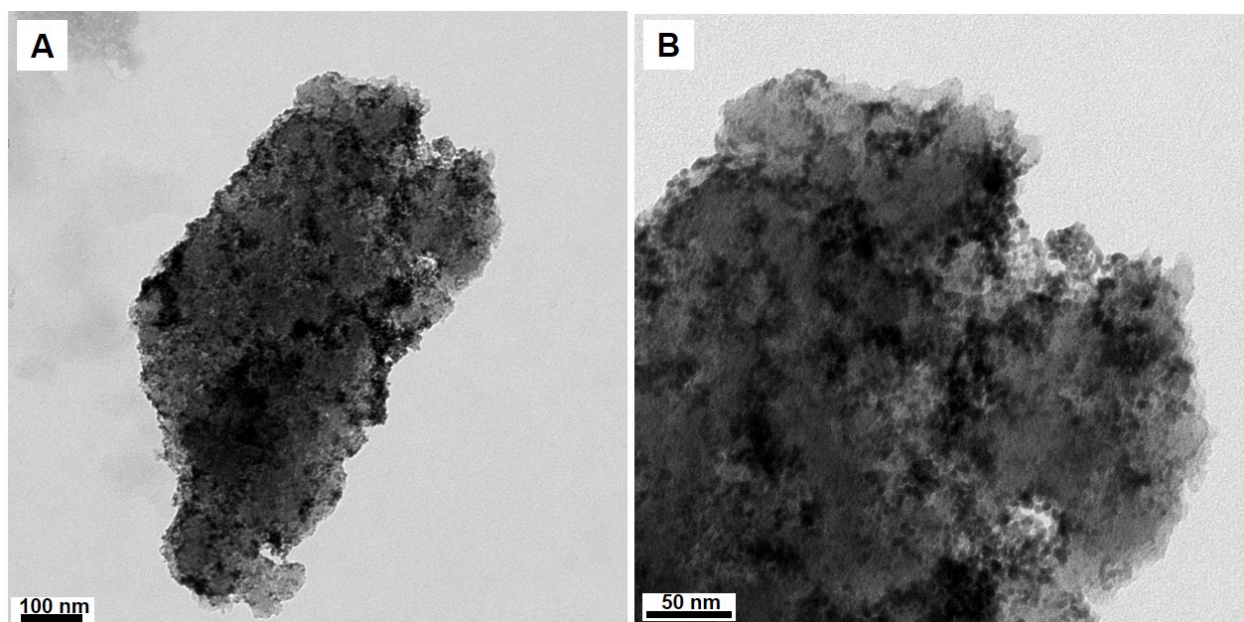


Figure S12. TEM images of commercial Pd/C catalyst used in this study. Sample obtained from Sigma Aldrich Chemicals (Atlanta, GA), Cat # 205699

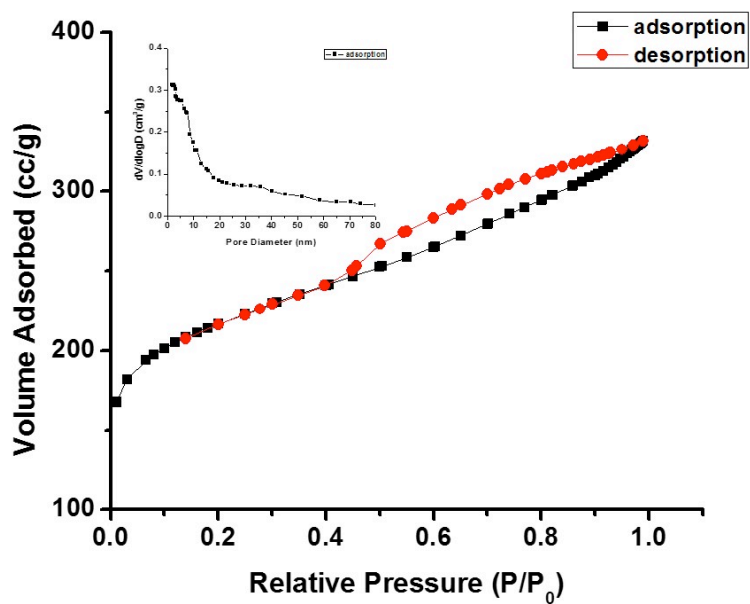


Figure S13. N_2 adsorption/desorption isotherm of commercial Pd/C catalyst. The inset shows the pore size distribution. The specific surface area (BET method) and pore volume (BJH method) were $762.2 \text{ m}^2/\text{g}$, $0.51 \text{ cm}^3/\text{g}$, and the average pore diameter was determined to be 2.6 nm.

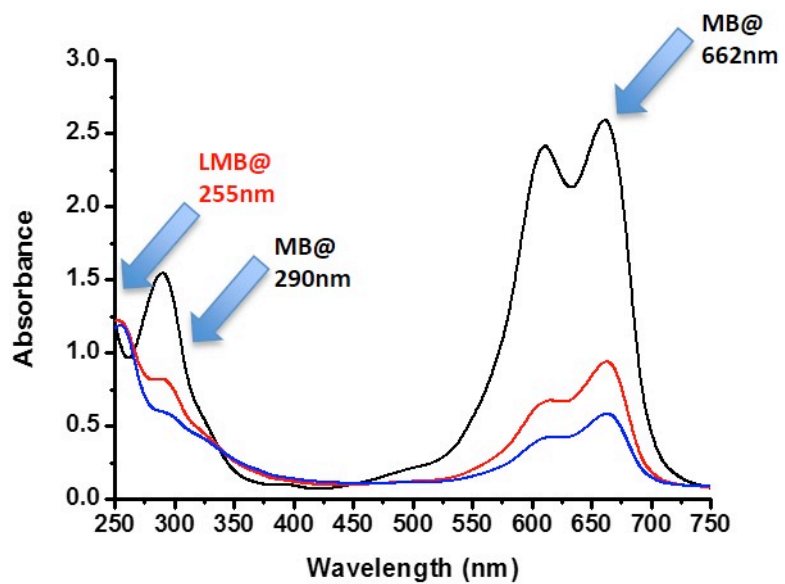


Figure S14. UV-visible absorbance spectra for the reduction of organic dye MB by NaBH₄. After the addition of MpSi-Pd nanoparticles, the absorption peaks for MB (290 nm and 650 nm) decreased and new band for Leuco-MB at 255nm appeared in the spectrum.

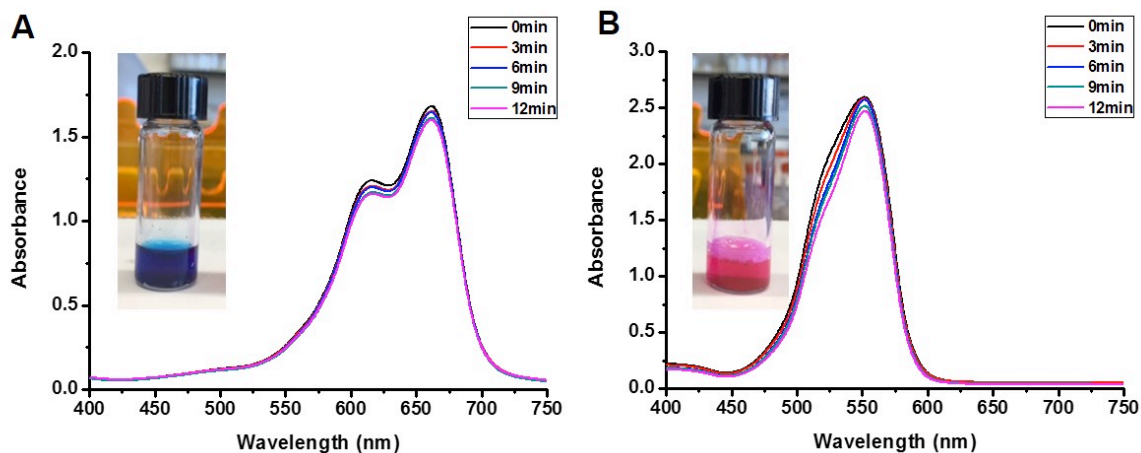


Figure S15. Time-dependent UV-visible absorbance spectra for the reduction of organic dyes by NaBH_4 , after the addition of MpSi nanoparticles (1mg/mL). No absorbance changes were detected within 12 mins for (A) methylene blue (MB) aqueous solution (1 mM) and (B) Rhodamine B (RhoB) aqueous solution (1 mM). Insets show photographs of the reaction mixtures 12 mins after the addition of the MpSi nanoparticles to the dye + NaBH_4 solutions.

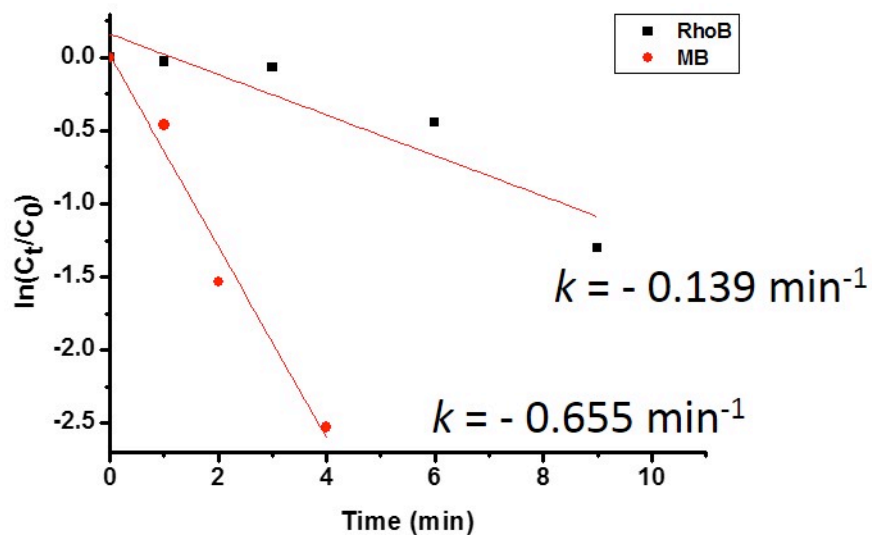


Figure S16. Plot of $\ln(C_t/C_0)$ versus time for reduction of the organic dyes methylene blue (MB) and rhodamine B (RhoB) by NaBH_4 , catalyzed by MpSi-Pd nanocomposite; ■ RhoB (1 mM) ; ● MB (1 mM). The rate constant k is estimated from the slope of straight line of $\ln(C_t/C_0)$ versus reaction time.